applied optics

High refractive index immersion liquid for superresolution 3D imaging using sapphire-based aplanatic numerical aperture increasing lens optics

Junaid M. Laskar,[1,*] P. Shravan Kumar,[2] Stephan Herminghaus,[1] Karen E. Daniels,[3] and Matthias Schröter[1,4]

[1]Max Planck Institute for Dynamics and Self-Organization (MPIDS), 37077 Göttingen, Germany
[2]Department of Physics, IIT Guwahati, Guwahati, Assam, India
[3]Department of Physics, NC State University, Raleigh, North Carolina 27695, USA
[4]Institute for Multiscale Simulation, Friedrich-Alexander-Universität Erlangen-Nürnberg, Erlangen, Germany
*Corresponding author: junaid.laskar@ds.mpg.de

Received 25 January 2016; revised 7 March 2016; accepted 14 March 2016; posted 15 March 2016 (Doc. ID 257589); published 12 April 2016

Optically transparent immersion liquids with refractive index ($n \sim 1.77$) to match the sapphire-based aplanatic numerical aperture increasing lens (aNAIL) are necessary for achieving deep 3D imaging with high spatial resolution. We report that antimony tribromide ($SbBr_3$) salt dissolved in liquid diiodomethane (CH_2I_2) provides a new high refractive index immersion liquid for optics applications. The refractive index is tunable from $n = 1.74$ (pure) to $n = 1.873$ (saturated), by adjusting either salt concentration or temperature; this allows it to match (or even exceed) the refractive index of sapphire. Importantly, the solution gives excellent light transmittance in the ultraviolet to near-infrared range, an improvement over commercially available immersion liquids. This refractive-index-matched immersion liquid formulation has enabled us to develop a sapphire-based aNAIL objective that has both high numerical aperture (NA = 1.17) and long working distance (WD = 12 mm). This opens up new possibilities for deep 3D imaging with high spatial resolution.

OCIS codes: (160.4670) Optical materials; (120.4530) Optical constants; (120.5710) Refraction; (110.6880) Three-dimensional image acquisition; (180.6900) Three-dimensional microscopy; (220.3620) Lens system design.

http://dx.doi.org/10.1364/AO.55.003165

1. INTRODUCTION

Sapphire-based aplanatic numerical aperture increasing lenses (aNAILs) [1,2] provide a promising route to achieve superresolution 3D imaging [3], but their development requires a suitable refractive-index-matching liquid ($n \sim 1.77$). A typical aNAIL design would include a truncated aplanatic solid immersion lens of plano–convex shape, made of high refractive index solid material [4–6], such as sapphire [7,8]. To date, the lack of a suitable immersion liquid has limited the application of aNAIL to subsurface microscopy of objects immersed inside a refractive-index-matched solid medium, without the possibility of depth scanning [1,2,6]. Therefore, a refractive-index-matched immersion liquid will allow for simultaneously harnessing both the high spatial resolution and the depth scanning capability of sapphire-based aNAILs [3]. However, a persistent challenge in the search for high refractive index immersion liquids is to find one with both low absorbance and low scattering. The ideal liquid would provide optical transparency across the full spectrum from ultraviolet to near-infrared, as well as tunability to provide precise index matching [9].

A promising candidate solvent is the organic liquid diiodomethane (CH_2I_2), which is one of the liquids with the highest known refractive index values ($n = 1.74$). While other high refractive index liquids exist (phenyldi-iodoarsine ($C_6H_5AsI_2$) with $n = 1.85$ and selenium monobromide (Se_2Br_2) with $n = 2.1$ [10]), diiodomethane has the key advantage of being commercially available. In addition, diiodomethane is an excellent solvent, and many liquid formulations using salts dissolved in diiodomethane are reported to increase the refractive index [10] and are even available commercially (Cargille Labs, Series M, $n = 1.8$). However, the strong light scattering and high absorbance of these formulations render them insufficiently transparent for high-resolution optics applications. A lack of knowledge of a salt formulation to increase the refractive index while maintaining optical transparency has caused diiodomethane to remain underutilized as a preferred immersion solvent liquid,

despite its inertness with many minerals (including sapphire) [10].

The refractive index of an optical medium is typically proportional to its mass density, as described by the Lorentz–Lorentz equation [11]; this suggests that salts containing heavy elements would be promising candidates. In addition, a large electronegativity difference between the salt cation and anion typically predicts improved solubility. Guided by these principles, we screened four different salts—antimony tribromide ($SbBr_3$) [10], antimony trichloride ($SbCl_3$), barium chloride ($BaCl_2$), and bismuth trichloride ($BiCl_3$)—as potential solutes in CH_2I_2. Of this list, $BaCl_2$ and $BiCl_3$ were found to have poor solubility due to small cation–anion electronegativity differences. Despite the excellent solubility of $SbCl_3$, the refractive index increased only by 0.02, due to the low atomic weight of chlorine. Therefore, only $SbBr_3$ was found to be a suitable candidate: for concentrations between 20 wt. % and saturation in liquid CH_2I_2, it achieves a refractive index as high as $n \sim 1.873$. In addition, this solution shows excellent optical transparency and low scattering in the wavelength ranges $\lambda < 350$ nm and 450 nm $< \lambda <$ 1060 nm. Below, we present measurements quantifying the concentration, temperature, and wavelength dependence of the index of refraction, transmittance, and scattering of these liquid solutions.

2. METHODS

We prepare liquid solutions of different concentrations (wt. %) from a powder sample of $SbBr_3$ (99% pure, Alfa Aesar) dissolved in the liquid CH_2I_2 (99% pure, Sigma-Aldrich). To obtain a solution of given wt. %, we mix the two components in the desired weight ratio, first on an electrical shaker for 6 h at $T = 22$°C and then in a centrifuge for 3 h at 800 rpm at $T = 15$°C. We then separate the upper (supernatant) liquid solution from the precipitate (assumed to contain chemical impurities) collected at the bottom of the centrifuge tube. For a 50 wt. % concentration at room temperature ($T = 22$°C), crystals are also formed that remain in equilibrium with the supernatant (saturated) solution. Note that the chemical handling of both components requires significant care. Antimony tribromide is harmful if swallowed (H302) or inhaled (H332), and is hygroscopic (absorbs water). Diiodomethane is harmful if swallowed (H302), causes skin irritation (H315), and serious eye damage (H318), and also may cause respiratory irritation (H335).

We perform index of refraction measurements using a liquid refractometer based on the design of Nemoto [12], as shown schematically in Fig. 1. The apparatus determines the displacement δ of a laser beam, due to passing through a liquid-filled cuvette rotated by an angle θ with respect to the beam. The center of the laser beam is determined by scanning a knife edge across its profile. As shown in the inset of Fig. 2, the light intensity profile $P(x)$ is well described by an error function, as expected for a single-mode laser. We identify the center of the beam as the location x at which $P(x)$ rises fastest, as obtained by numerical differentiation. Sample Gaussian beam profiles dP/dx are shown in Fig. 2, characterized by the beam width w at which the power falls by a factor of $1/e^2$ [13,14]. Throughout the measurements, we control the temperature of the liquid to ±0.05°C by encapsulating the quartz cuvette

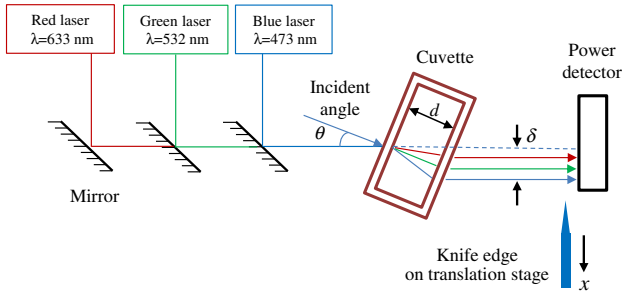

Fig. 1. Schematic of the liquid refractometer setup, based on the design of Nemoto [12]. The cuvette cross section is 20 mm × 10 mm, with optical measurements performed across the width $d = 10$ mm.

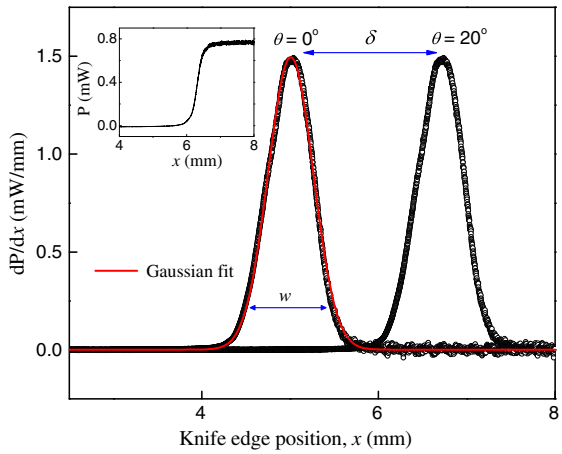

Fig. 2. Measurement of laser beam displacement δ by knife-edge scanning. The inset shows the measured power versus the knife position. The main plot shows fits to two Gaussian beam profiles (i.e., derivatives of the inset) for the angles $\theta = 0°$ and 20°. The difference between the two maxima is the displacement $\delta(20°)$.

(Hellma Analytics) inside a rectangular copper block containing channels connected to a refrigerated water bath circulator (Neslab RTE 111). The copper block is mounted on a rotation stage with a vernier scale, which provides an angular reproducibility of ±5 arc min.

Following Nemoto [12], the refractive index n of the liquid can be calculated from

$$n = n_0 \sin\theta \sqrt{1 + \left[\frac{\cos\theta}{\sin\theta - \Delta/d}\right]^2}, \quad (1)$$

where n_0 is the refractive index of air (the empty cuvette), d is the width of the cuvette, and $\Delta \equiv \delta - \delta_0$ is the relative displacement of the Gaussian peak for the liquid-filled cuvette relative to the empty cuvette.

To obtain n, we repeat the same measurement at seven different incident angles $\theta = (\pm 10°, \pm 20°, \pm 30°, +40°)$, corresponding to both clockwise and counterclockwise rotation of the cuvette with respect to the incident light. The average of these seven measurements provides the value of n for each combination of wavelength, temperature, and $SbBr_3$ concentration. We repeat this process for three wavelengths of light ($\lambda = 473, 532$, and 633 nm), five temperatures from 15°C

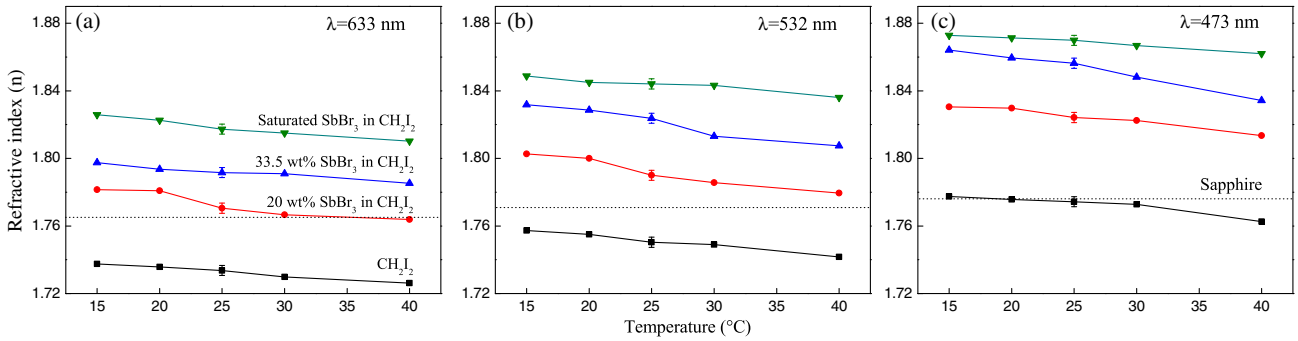

Fig. 3. Refractive indices of both pure diiodomethane (black lines) and with dissolved antimony tribromide (colored lines). Each panel compares the results for a single wavelength, as a function of concentration and temperature. The refractive index for ordinary rays through sapphire is shown by dotted line for comparison.

to 40°C, and three concentrations (20 wt. %, 33.5 wt. %, and saturation concentration).

Equation (1) already reduces systematic errors due to geometric imperfections of the cuvette by measuring all values of δ against the empty cuvette. In addition, we have analyzed the systematic errors in our setup and determined that the precision of the rotation stage and the imperfect parallelism of the cuvette sidewalls are the largest sources of error. These combined effects result in a refractive index measurement error of ± 0.003. In practice, we find that we are able to measure the refractive index of water and ethanol to within ± 0.001 of values reported in the literature [15–17].

3. RESULTS

A. Index of Refraction

We find that $SbBr_3$ dissolved in CH_2I_2 can meet and exceed the index of refraction of sapphire over a broad range of temperatures, visible wavelengths, and concentration greater than 20 wt. %. Figure 3 presents the measured values of n as a function of wavelength [panels (a)–(c)], temperature (plot abscissa), and concentration (line series). In each case, the refractive index can be increased by either changing the concentration (more dissolved salt corresponds to higher n) or the temperature (higher temperature decreases n). In applications, preparing a solution of known concentration is more convenient for coarse tuning, and temperature is more convenient for fine tuning *in situ*. The largest value we measure is $n = 1.873$, for saturated solutions at low temperature and short wavelength.

B. Optical Transparency

Optical transparency, which can be degraded by both light scattering and absorption, plays a crucial role in determining the utility of an immersion liquid. We characterize these properties of the $SbBr_3$–CH_2I_2 solutions, and compare with the two commonly used commercial high refractive index immersion liquids (Cargille M Series with $n = 1.71 \pm 0.0005$ and $n = 1.80 \pm 0.0005$). Figure 4 shows the transmittance spectra, measured from the near-ultraviolet to the near-infrared. The illumination source is an Ocean Optics tungsten-halogen light source (Model HL-2000-FHSA-LL with output power 4.5 mW) and transmitted light is recorded on an Ocean Optics spectrometer (Model HR2000 +). For all five liquid solutions, there is a significant absorption band centered around 410 nm (blue). In addition, there are several coincident absorption bands located at $\lambda = 725, 887$, and 1037 nm, which possibly arise due to the common solvent CH_2I_2 used for all five liquids.

Furthermore, we observe a Tyndall effect at all the three wavelengths, with stronger scattering for the Cargille liquids than for our $SbBr_3$ solutions. This suggests that Mie scattering is present, caused by colloidal particles with a size of the same order as λ [18]. In order to quantify the amount of scattering, we measure the relative increase in beam width $\Delta w = \frac{w - w_0}{w_0}$, where w and w_0 are the beam widths for the liquid and air-filled cuvettes, respectively. A large value of Δw signifies stronger scattering. For simplicity, all measurements are done at $T = 25$°C and for normal incidence ($\theta = 0°$), using the knife-edge scanning method shown in Fig. 2. Results for the two wavelengths 473 and 633 nm are given in Table 1.

At $\lambda = 633$ nm, the beam width remains unaffected for the $SbBr_3$–CH_2I_2 liquid solutions and the Cargille liquid $n = 1.71$. Only the Cargille $n = 1.80$ liquid contains colloidal particles in the relevant size range. At $\lambda = 473$ nm, the beam width also shows a concentration-dependent increase for the $SbBr_3$ - CH_2I_2 liquid solutions. A likely source of particles

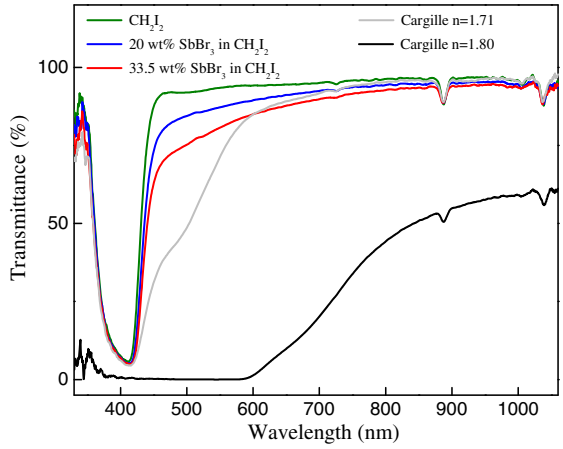

Fig. 4. Transmittance as a function of wavelength for a cuvette of width $d = 10$ mm.

Table 1. Proportional Increase (%) in the Beam Width, Referenced Against an Empty Cuvette

	Beam Width Increase (%)	
Liquid/Liquid Solution	$\lambda = 633$ nm	$\lambda = 473$ nm
Diiodomethane (CH_2I_2)	0	2.2
20 wt. % $SbBr_3$ solution	0	9.5
33.5 wt. % $SbBr_3$ solution	0	10.6
Cargille liquid ($n = 1.71$)	1.2	16
Cargille liquid ($n = 1.80$)	13.5	Opaque

in this diameter range is that hydrolysis with atmospheric humidity produces small antimony oxide crystals via the reaction $2SbBr_3 + 3H_2O \rightarrow Sb_2O_3 + 6HBr$ [19]. At the same wavelength, the Cargille liquid $n = 1.71$ shows an even stronger scattering, while the opacity of the $n = 1.8$ Cargille liquid does not even allow the measurement of the beam width.

C. Physical Properties

We characterize the volumetric thermal expansion coefficient (γ) and the density (ρ) of the liquid solution ($SbBr_3 + CH_2I_2$) as a function of concentration, using a dilatometer (PHYWE Systeme GmbH) and pycnometer (BRAND GmbH), respectively. We observe that decreasing the concentration of $SbBr_3$ from the saturated case increases γ by 50% and decreases ρ by 4%, as shown in Table 2. Because $SbBr_3$ reacts with H_2O, the liquid solution ($SbBr_3 + CH_2I_2$) is immiscible in water (see Section 3.B for details).

4. DISCUSSION

Antimony tribromide ($SbBr_3$) dissolved in diiodomethane (CH_2I_2) is a strong candidate as an immersion liquid for sapphire-based aNAIL lenses [see Fig. 5(a)]. Together with a refractive-index-matched immersion liquid, these lenses allow for the simultaneous increase of both the numerical aperture (NA, the light-gathering power) and the working distance (WD) of an objective lens [2,3]. This technique places the object of interest at the aplanatic point of the spherical surface of the aNAIL lens in order to have an aberration-free focal spot. It can increase the NA of the backing objective lens by a factor of n_{aNAIL}^2, up to the maximum achievable value n_{aNAIL} [1,2].

Figure 5(b) shows the picture of the aNAIL and the backing objective lens system designed for significantly increasing the numerical aperture of the backing objective lens from

Table 2. Physical Properties of the Liquid Solutions of Different Concentrations[a]

Liquid Solution	Thermal Expansion Coefficient, γ(K^{-1})	Density, ρ (gm/mL)
20 wt. % $SbBr_3$ solution	6.9×10^{-4}	3.422
33.5 wt. % $SbBr_3$ solution	5.4×10^{-4}	3.504
Saturated $SbBr_3$ solution	4.6×10^{-4}	3.572

[a]All density measurements were performed at $T = 22$°C. The temperature ranges, over which the volumetric thermal expansion measurements were performed, were $T = 23$–35°C, 20–32°C and 25–36°C for 20 wt. %, 33.5 wt. %, and saturated solution, respectively.

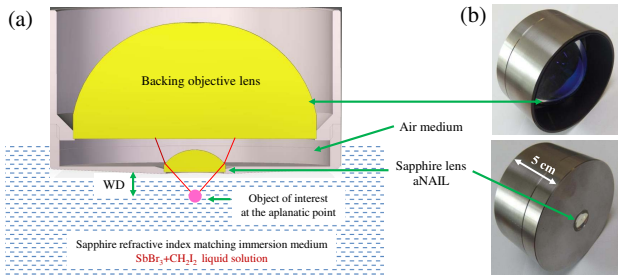

Fig. 5. (a) Schematic of the design for simultaneous increase of NA and WD, using a sapphire-based aNAIL lens system immersed in the refractive index matching liquid (solution of $SbBr_3$ in CH_2I_2). (b) Picture of an aNAIL and backing objective lens system, designed to have NA = 1.17 and WD = 12 mm.

0.619 to 1.17, while still maintaining a long working distance (WD = 12 mm). The lens system was designed using WinLens3D optical design software.

Because n is tunable via both concentration and temperature, the liquid formulation presented here could open new routes to creating adaptive lenses with tunable optical power [20]. In these applications, liquid lenses have the advantage of additionally allowing the *shape* of the lens to be tuned in order to adjust its focal length (and therefore the optical power), mimicking the mechanism of the human eye. To date, the lack of an appropriate high-n liquid has limited the range of tunable optical power, as this depends on the difference of the refractive indices of the two immiscible liquids used to build the adaptive liquid lens [21–23].

Finally, we close with the application that inspired our work on this immersion liquid formulation: the imaging of gems made from corundum minerals (ruby and sapphire), which have $n \sim 1.77$. High spatial resolution lenses such as those described above (aNAIL) would open new routes to studying the crystallization process during mineral formation [24] and quality in the manufacturing industry (gemstone, watch, etc.) [25]. Importantly, ruby also has a pressure-dependent fluorescence peak [26–28], which has recently been exploited as a tool for measuring the pressure field inside rubies themselves [29,30].

5. CONCLUSION

We have demonstrated that antimony tribromide ($SbBr_3$) dissolved in diiodomethane (CH_2I_2), for concentrations between 20 wt. % and saturation, provides a promising new high refractive index liquid formulation. At standard conditions for temperature and pressure and at wavelengths from near-ultraviolet to near-infrared, we observe that $n > 1.77$ (sapphire) is attainable. For optimized choice of parameters (low temperature, short wavelength, high concentration), we can achieve $n = 1.873$. In addition, this liquid is observed to have high transmission and low scattering for $\lambda < 350$ nm and $\lambda \gtrsim 450$ nm. On using this liquid formulation as a refractive-index-matched immersion medium, we have developed a sapphire-based aplanatic numerical aperture increasing lens that has both high numerical aperture NA = 1.17 and long working distance (WD = 12 mm). This paves the way for deep 3D imaging

with high spatial resolution. Moreover, the tunability of this extremely high n liquid has several other promising applications, particularly in the development of adaptive liquid lens, gemstone, watch industry, etc.

Funding. Alexander von Humboldt Foundation; James S. McDonnell Foundation; FOKOS (Ludwig Prandtl stipend).

Acknowledgment. The authors would like to thank Markus Benderoth and Kristian Hantke for invaluable technical expertise. In addition, K. E. D. is grateful to the Alexander von Humboldt Foundation and the James S. McDonnell Foundation for their financial support. P. S. K. is grateful to the FOKOS society for providing him with a Ludwig Prandtl stipend.

REFERENCES

1. S. B. Ippolito, B. Goldberg, and M. Ünlü, "High spatial resolution subsurface microscopy," Appl. Phys. Lett. **78**, 4071–4073 (2001).
2. S. Ippolito, B. Goldberg, and M. Ünlü, "Theoretical analysis of numerical aperture increasing lens microscopy," J. Appl. Phys. **97**, 053105 (2005).
3. K. A. Serrels, E. Ramsay, P. A. Dalgarno, B. Gerardot, J. O'Connor, R. H. Hadfield, R. Warburton, and D. Reid, "Solid immersion lens applications for nanophotonic devices," J. Nanophoton. **2**, 021854 (2008).
4. S. M. Mansfield and G. Kino, "Solid immersion microscope," Appl. Phys. Lett. **57**, 2615–2616 (1990).
5. Y. Lu, T. Bifano, S. Ünlü, and B. Goldberg, "Aberration compensation in aplanatic solid immersion lens microscopy," Opt. Express **21**, 28189–28197 (2013).
6. K. Agarwal, R. Chen, L. S. Koh, C. J. Sheppard, and X. Chen, "Crossing the resolution limit in near-infrared imaging of silicon chips: targeting 10-nm node technology," Phys. Rev. X **5**, 021014 (2015).
7. Q. Wu, R. D. Grober, D. Gammon, and D. Katzer, "Imaging spectroscopy of two-dimensional excitons in a narrow GaAs/AlGaAs quantum well," Phys. Rev. Lett. **83**, 2652–2655 (1999).
8. E. S. Lee, S.-W. Lee, J. Hsu, and E. O. Potma, "Vibrationally resonant sum-frequency generation microscopy with a solid immersion lens," Biomed. Opt. Express **5**, 2125–2134 (2014).
9. M. Deetlefs, K. R. Seddon, and M. Shara, "Neoteric optical media for refractive index determination of gems and minerals," New J. Chem. **30**, 317–326 (2006).
10. R. Meyrowitz, "A compilation and classification of immersion media of high index of refraction," Am. Mineral. **40**, 398–409 (1955).
11. F. Lamelas, "Index of refraction, density, and solubility of ammonium iodide solutions at high pressure," J. Phys. Chem. B **117**, 2789–2795 (2013).
12. S. Nemoto, "Measurement of the refractive index of liquid using laser beam displacement," Appl. Opt. **31**, 6690–6694 (1992).
13. P. B. Chapple, "Beam waist and m2 measurement using a finite slit," Opt. Eng. **33**, 2461–2466 (1994).
14. J. Magnes, D. Odera, J. Hartke, M. Fountain, L. Florence, and V. Davis, "Quantitative and qualitative study of Gaussian beam visualization techniques," arXiv:physics/0605102 (2006).
15. P. Schiebener, J. Straub, J. L. Sengers, and J. Gallagher, "Refractive index of water and steam as function of wavelength, temperature and density," J. Phys. Chem. Ref. Data **19**, 677–717 (1990).
16. A. Zaidi, Y. Makdisi, K. Bhatia, and I. Abutahun, "Accurate method for the determination of the refractive index of liquids using a laser," Rev. Sci. Instrum. **60**, 803–805 (1989).
17. E. Moreels, C. De Greef, and R. Finsy, "Laser light refractometer," Appl. Opt. **23**, 3010–3013 (1984).
18. C. F. Bohren and D. R. Huffman, *Absorption and Scattering of Light by Small Particles* (Wiley, 2008).
19. D. R. Lide, *Handbook of Chemistry and Physics: A Ready-Reference Book of Chemical and Physical Data 2012-2013* (CRC Press, 2012).
20. H. Ren, D. Fox, P. A. Anderson, B. Wu, and S.-T. Wu, "Tunable-focus liquid lens controlled using a servo motor," Opt. Express **14**, 8031–8036 (2006).
21. L. Li, Q.-H. Wang, and W. Jiang, "Liquid lens with double tunable surfaces for large power tunability and improved optical performance," J. Opt. **13**, 115503 (2011).
22. S. Kuiper and B. Hendriks, "Variable-focus liquid lens for miniature cameras," Appl. Phys. Lett. **85**, 1128–1130 (2004).
23. K. Mishra, C. Murade, B. Carreel, I. Roghair, J. M. Oh, G. Manukyan, D. van den Ende, and F. Mugele, "Optofluidic lens with tunable focal length and asphericity," Sci. Rep. **4**, 6378 (2014).
24. H. R. Wenk and A. Bulakh, *Minerals: Their Constitution and Origin* (Cambridge University, 2004).
25. R. W. Hughes, *Ruby & Sapphire* (Rwh Pub, 1997).
26. H. Mao, J. Xu, and P. Bell, "Calibration of the ruby pressure gauge to 800 kbar under quasi-hydrostatic conditions," J. Geophys. Res. **91**, 4673–4676 (1986).
27. W. B. Holzapfel, "Refinement of the ruby luminescence pressure scale," J. Appl. Phys. **93**, 1813–1818 (2003).
28. K. Syassen, "Ruby under pressure," High Pressure Res. **28**, 75–126 (2008).
29. Y. Chen, A. Best, T. Haschke, W. Wiechert, and H.-J. Butt, "Stress and failure at mechanical contacts of microspheres under uniaxial compression," J. Appl. Phys. **101**, 084908 (2007).
30. Y. Chen, A. Best, H.-J. Butt, R. Boehler, T. Haschke, and W. Wiechert, "Pressure distribution in a mechanical microcontact," Appl. Phys. Lett. **88**, 234101 (2006).